Available online at www.sciencedirect.com
ScienceDirect
Journal of Solid State Chemistry 180 (2007) 2102–2109
JOURNAL OF SOLID STATE CHEMISTRY
www.elsevier.com/locate/jssc

Synthesis of new mixed valence compounds $MV^{5+}V_2^{4+}O_7$(M = NH_4, K): Crystal structure of $NH_4V_3O_7$ and electrical properties of KV_3O_7

J.C. Trombe*, O. Szajwaj, Ph. Salles, Jean Galy

Centre d'Elaboration de Matériaux et d'Etudes Structurales (CEMES/CNRS), 29 rue Jeanne Marvig, BP 94347, 31055 Toulouse cedex, France

Received 17 January 2007; received in revised form 19 April 2007; accepted 24 April 2007
Dedicated to Pr. Joachim Strähle for his 70th birthday
Available online 8 May 2007

Abstract

A new mixed valence compound, $NH_4V_3O_7$, as single crystals, has been synthesized hydrothermally. It crystallizes in the monoclinic system, space group I2/m with lattice parameters $a = 12.198(1)$ Å, $b = 3.7530(2)$ Å, $c = 13.178(1)$ Å, $\beta = 100.532(6)^\circ$, $V = 593.11(7)$ Å^3, $Z = 4$. The crystal structure determined with $R = 0.038$ consists of $(V_3O_7)_n$ layers linked by ammonium cations. The layer is built up by replication through symmetry elements of three independent distorted octahedra sharing edges and corners. The distortion of vanadium octahedra tends to vary and the coordination number CN is reasonably selected as equal to 5+1. KV_3O_7, synthesized by the mild hydrothermal route as a largely pure phase, is isostructural and its semi-conductive character is indicative of the presence of V^{4+} and V^{5+} sites. These are mixed valence compounds $MV^{5+}V_2^{4+}O_7$, the vanadium localization on three independent crystallographic sites enabling their electric behavior by electron hopping.

Keywords: Ammonium; Potassium vanadium mixed valence oxide; Hydrothermal synthesis; Structure; Conductivity

1. Introduction

Vanadium oxide bronzes with their mixed valence networks $[V_xO_y]$ containing the $V^{5+}-V^{4+}$ or $V^{4+}-V^{3+}$ couples exhibit a wide range of crystal structures whose electrical balance of the ionocovalent network is directly linked to the amount of inserted or intercalated elements—alkalis, alkaline earths or metals. Wadsley was the first to demonstrate in 1955 that the β $Na_xV_2O_5$ type vanadium bronze presents a three-dimensional $[V_2O_5]_n$ network in which non-stoichiometric amounts of sodium are inserted within "living" tunnels [1]. Formally this phase can be written $Na_xV_{2-x}^{5+}V_x^{4+}O_5$ and shows an homogeneity range for $0.2<x<0.33$. Its structure is common to a wide range of phases containing all alkalis, alkaline-earths, Cu, Ag, Cd and Pb cations. More recently, another tunnel structure has been observed in the vanadium–molybdenum mixed bronze $A_x(Mo,V)_8O_{21}$ with $A = K^+, Rb^+, Cs^+$ [2]. Again Wadsley was a precursor with his research on the lithium vanadium bronze $Li_{1+x}V_{3-x}^{5+}V_x^{4+}O_8$ family which plays such an important part for batteries as an electrode [3]. This bronze shows a layer structure in which $[V_3O_8]_n$ layers are held together via a certain amount of lithium atoms intercalated between them. Similarly, oxides with potential applications in rechargeable batteries, were researched and the bronze $Cu_{2.33-x}V_4O_{11}$, exhibits a new layer structure, with an outstanding reversible extrusion–insertion of Cu atoms between the $[V_4O_{11}]_n$ layers [4]. $M_xV_2O_5$ bronze structures and the various resultant phases due to the crystallographic shearing mechanism of the ionocovalent network have been reviewed [5,6].

The hydrothermal method has proven to be highly efficient for the preparation of new open frameworks [7–15]. However some additional material can thus be prepared, namely a pure monoclinic $V_{1.1}Mo_{0.9}O_5$ where vanadium atoms present the two oxidation states, either (IV) or (V) [16]. This compound cannot be synthesized by solid state reaction as a pure one. While looking for an oxy-fluoride copper–vanadium compound synthesized by the hydrothermal method, we came across a tiny crystal of $NH_4V_3O_7$ mixed with a large quantity of the compound

*Corresponding author.
E-mail address: trombe@cemes.fr (J.C. Trombe).

0022-4596/$ - see front matter © 2007 Elsevier Inc. All rights reserved.
doi:10.1016/j.jssc.2007.04.024

known $(NH_4)_2VO(V_2O_7)$ [17,18]. Here the structure of $NH_4V^{5+}V_2^{4+}O_7$ is detailed. Since the ammonium size is comparable to that of potassium, we successfully substituted potassium for ammonium ions, using the hydrothermal synthesis. However, the potassium compound can be prepared generally by solid state reaction: in fact $K_2VO(V_2O_7)$ prepared by this technique [19] is isostructural with $(NH_4)_2VO(V_2O_7)$. We failed to synthesize KV_3O_7 by the solid state route. A possible explanation will be given.

2. Experimental

2.1. Synthesis

The ammonium title compound was synthesized hydrothermally under autogenous pressure. An aqueous suspension (5 mL) of NH_4VO_3 (3.80 mmol), $CuCO_3.Cu(OH)_2$ (0.47 mmol) and NH_4F (3.77 mmol) was heated at 200 °C for three weeks in a teflon-lined stainless steel autoclave. After cooling down at room temperature, the pH of the final solution was found to be equal to 8.7 and the resulting product, shape like black tangled crystals, was filtered, washed with distilled water and dried at room temperature.

The first crystal, a thin platelet, corresponded to $(NH_4)_2V_3O_8$ [17] according to the system found (tetragonal) and the cell parameters observed ($a = b = 8.9053(3)$ Å and $c = 5.5774(2)$ Å). Furthermore, X-ray powder analysis of the bulk of this compound carried out with a Siemens XRD 3000 TT diffractometer using Cu Kα radiation ($\lambda = 1.5418$ Å) indicated a mixture of phases: a major phase, $(NH_4)_2V_3O_8$ (PDF-2 No. 78-1229) mixed with very small amounts of CuV_2O_5 (PDF-2 No. 43-80) and $NH_4V_3O_7$ (this work).

The second crystal, a needle, was completely different (monoclinic system with $a = 12.198(1)$ Å, $b = 3.7530(2)$ Å, $c = 13.178(1)$ Å and $\beta = 100.532(6)^\circ$). To our knowledge, such data does not seem to be present within the system H, N, O, F, V and Cu. Therefore, the compound structure was determined and its formula found to be $NH_4V_3O_7$.

First we tried to optimize the amount of the $NH_4V_3O_7$ phase by hydrothermal synthesis through different reactions varying the reactant ratio of $NH_4VO_3/Cu(CO_3).Cu(OH)_2/NH_4F$. Only a molar ratio of these last reactants of 4/0.5/8 resulted in a mixture of phases of approximately 60% of $(NH_4)_2V_4O_9$ (PDF-2 No. 23-791) and about 40% of $NH_4V_3O_7$. However under the reaction conditions chosen, it seems impossible to go further and to obtain the pure $NH_4V_3O_7$ phase.

Considering the stoichiometry of the $NH_4V_3O_7$ formula, a mixture of two vanadium (IV) and one vanadium (V) were needed which would react upon one cation such as NH_4^+ or the alkalis or silver. Vanadium (V) to (IV) can be easily reduced by a weighted amount of oxalic acid [20]. Therefore, a mixture of V_2O_5 (3/2 mmol), $H_2C_2O_4$, $2H_2O$ (1 mmol) and M_2O or M_2CO_3 (1/2 mmol, $M =$ ammonium, alkalis and silver) in water (5 ml) was heated at 200 °C for some days. According to its X-ray powder pattern, only the potassium was successful and it depended greatly on heating time. The cell constants of the phase KV_3O_7, practically pure (heating 45 days), are given in Table 1. It is worthwhile noticing a major decrease of a, c and β cell parameters in the potassium compound compared to those of ammonium; in both cases the b axis stays practically constant.

With respect to potassium, attempts have also been made using solid-state chemistry. A mixture of stoichiometric KVO_3 (1 mmol) and V_2O_4 (1 mmol) was ground, placed in a silica tube sealed under primary vacuum and heated at a rate of 2.5°/mn up to 450 °C for 12 h. After cooling to room temperature, the resulting compound was studied by powder X-ray diffraction. Further grinding and annealing at 550, 650 and 800 °C, was carried out. In all cases, a mixture of phases was observed: $K_2V_3O_8$ (PDF-2 No. 51-1732) plus V_2O_4 (PDF-2 No. 19-1398).

Part of the KV_3O_7 compound, synthesized by the hydrothermal method, was heated at 500 °C and then at 650 °C under vacuum. After heating at 500 °C, the compound remained stable; only a contraction of volume

Table 1
Crystallographic data for the MV_3O_7 phases with $M = NH_4$, K

	NH_4	K
Crystal data		
System	monoclinic	monoclinic
Space group	I2/m	I2/m
a (Å)	12.198(1)	11.974(4)
b (Å)	3.7530(2)	3.756(1)
c (Å)	13.178(1)	12.812(3)
β (°)	100.532(6)	98.29(2)
V (Å^3)	593.11(7)	570.2(3)
Z	4	
Formula weight	282.86	
$\rho_{calc.}$ (g/cm^3)	3.168	
$\mu_{MoK\alpha}$ (cm^{-1})	46.19	
Transmission coefficient range	min = 0545 * max = 0.814	
Morphology	needle	
Crystal size (mm)	0.25 * 0.04 * 0.04	
Color	black	
Experimental details		
Wavelength (MoKα)	0.71073	
Monochromator	graphite	
Max. Bragg angle θ (°)	30	
Collected reflections	3422	
Data(I < 2s(I))/restraints/ parameters	870/0/67	
$R_{obs.}$	0.0376	
$w_{Robs.}$	0.0956	
Goodness of fit on F^2	1.081	
Weighting scheme	0.0406/5.2109	
Δ/ρ_{max}	0.778	
Δ/ρ_{min}	−1.119	

was noted: from 570.2(3) to 567.9(7) Å^3. After heating at 650 °C, it slowly turned into a mixture of $K_2V_3O_8$ and V_2O_4 phases. Then, it becomes clear why KV_3O_7 cannot be synthesized by solid-state reaction, owing to the great stability of $K_2V_3O_8$ in the presence of V_2O_4.

2.2. Spark plasma sintering

Ceramic pellets of the KV_3O_7 phase were obtained using Spark plasma sintering with a Sumitomo 2080 machine installed by CEMES for the "Plate-forme Nationale de Frittage Flash /CNRS" in Toulouse.[1] For the KV_3O_7 pellet, a weighed amount of powder was placed in 8 mm inner diameter carbon die to achieve a 3 mm-thick high ceramic. The pellet, under a uniaxial pressure of 50 MPa was heated with 3 ms DC electric pulses as follows: 20–500 °C in 5 min, 500–600 °C in 2 min followed by 2 min isothermal holding time at 600 °C and 50 MPa before rapid quenching. The compaction of the pellets obtained was in excess of 95%. Pellets were controlled by XRD and checked to match the nominal powder.

2.3. Electrical resistivity

Platinum wires were glued to the sintered KV_3O_7 pellet using platinum conducting paint, and the electrical resistivity was measured on the basis of the four-probe direct current method using a Keithley (224 and 181) coupled apparatus in the $300 < T(K) < 750$ temperature range. To prevent oxidation of *V*, all measurements were carried out under helium. Measurement cycles were repeated at least twice to confirm the reproducibility of the results.

2.4. Crystal structure determination

A crystal of the ammonium title compound was selected using a binocular. Diffraction data were collected on an Enraf Nonius four circle diffractometer equipped with a Kappa-CCD detector using graphite-monochromatized MoKα radiation at 293 K. Intensity data were corrected for absorption using a numerical technique [21]. The structure solution was easily determined by direct methods, SIR92 [22]. Refinements were carried out using anisotropic thermal displacements of all non-hydrogen atoms by SHELXL-97 [23]. Hydrogen atoms pertaining to the ammonium ion were easily found through the Fourier difference method and they were introduced as riding on the nitrogen atom. The sets of physical crystallographic characteristics as well as the experimental conditions for $NH_4V_3O_7$ are given in Table 1.

[1]PNF2/CNRS – MHT, Université Paul Sabatier, Toulouse, France. Created by P. Millet, P. Rozier, J. Galy, 2003–2004.

Table 2
Atomic coordinates and thermal parameters in $NH_4V_3O_7$

Atoms	*x*	*y*	*z*	Ueq. (Å^2)
V1	0.65468(6)	1/2	0.20350(6)	0.00844(2)
V2	0.61794(7)	1/2	−0.05569(6)	0.0126(2)
V3	0.71508(6)	1/2	0.43933(5)	0.00717(2)
O1	0.5944(3)	1/2	0.3134(2)	0.0121(6)
O2	0.7443(3)	1/2	0.0724(2)	0.0087(6)
O3	0.8053(2)	1/2	0.3010(2)	0.0075(6)
O4	0.5307(3)	1/2	0.1039(3)	0.0153(7)
O5	0.8653(3)	1/2	0.5229(2)	0.0105(6)
O6	0.6710(4)	1/2	−0.1608(3)	0.0236(8)
O7	0.6325(3)	1/2	0.5219(3)	0.0180(7)
N	0.4172(4)	0	0.3290(4)	0.0255(10)
H1	0.488	0	0.314	0.03
H2	0.400	0.187	0.368	0.03
H3	0.362	0	0.272	0.03

Table 3
Selected bond lengths (Å) and angles (°) in $NH_4V_3O_7$

V1−O1	1.740(3)	V3−O7	1.612(3)
V1−O2	2.207(3)	V3−O3	2.295(3)
V1−O3	2.040(3)	V3−O1	2.007(3)
V1−O4	1.812(3)	V3−O5	1.957(3)
V1−O3*b* (x2)	1.9427(8)	V3−O2*b* (x2)	1.9541(9)
⟨V1−O⟩	1.947	⟨V3−O⟩	1.963
V2−O6	1.632(4)	V1−V3	3.060(1)
V2−O4	2.524(4)	V1−V2	3.363(1)
V2−O2	2.067(3)	V1−V1*b*	3.064(1)
V2−O4*a*	1.808(3)	V2−V2*a*	3.461(2)
V2−O5*b* (x2)	1.9281(7)	V3−V2*b*	2.980(1)
⟨V2−O⟩	1.981		
		NH4−NH4*e*	4.624(8)
		NH4−NH4*d*	4.59(1)

Hydrogen bonding

A−H…*D*	*D*−H	H…*A*	*A*…*D*	*D*−H…*A*
N−H1…O1 (x2)	0.91	2.29	2.898(4)	124.0
N−H2…O7*d* (x2)	0.92	1.96	2.861(4)	166.4
N−H3…O6*a* (2)	0.92	2.37	2.953(5)	121.5

The symmetry codes are given in Fig. 1.

The final atomic and equivalent thermal parameters with estimated standard deviations are shown in Table 2. Selected bond lengths and angles are given in Table 3.

3. Results

3.1. Structure description

$NH_4V_3O_7$, a formula derived from the structure determination is a mixed valence compound, i.e., $NH_4V^{5+}V_2^{4+}O_7$. A projection of the structure onto the (0 1 0) plane is shown in Fig. 1. All non-hydrogen atoms are located in the mirror planes of the space group I2/m at $y = 0$ and $y = \frac{1}{2}$; two hydrogen atoms of the NH_4^+ cation,

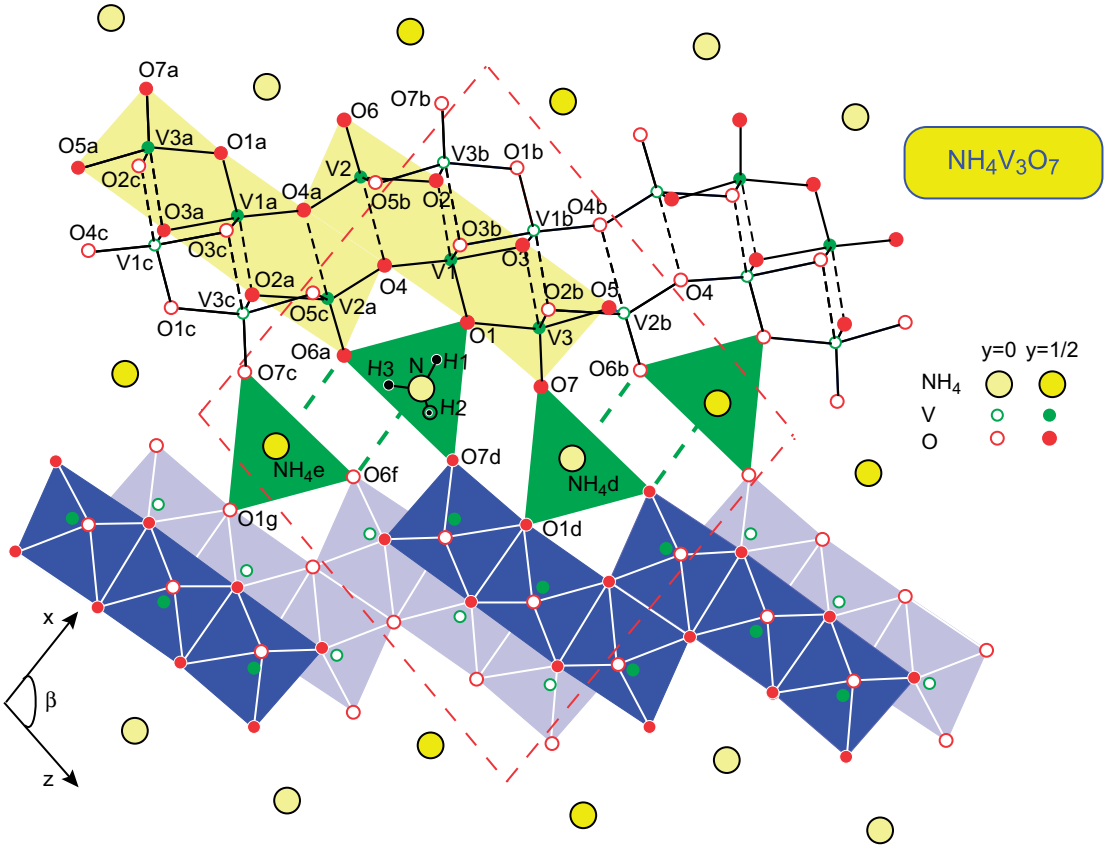

Fig. 1. Projection of $NH_4V_3O_7$ structure onto the plane (0 1 0) together with ball and spoke indications. The layer of VO_6 octahedra is schematized as heavy blue shading for octahedra centered in $y = \frac{1}{2}$ and light blue for those in $y = 0$. Symmetry operations: (a) $1-x, y, -z$; (b) $3/2-x, 1/2-y, 1/2-z$; (c) $-1/2+x, 1/2-y, -1/2+z$; (d) $1-x, y, 1-z$; (*e*) $1/2-x, 1/2+y, 1/2-z$; (f) $-1/2+x, -1/2+y, 1/2+z$; (g) $1/2-x, 1/2-y, 1/2-z$.

H1 and H3 lie as nitrogen in the mirror plane H2 being outside. The basic unit of the $NH_4V_3O_7$ is built up by three independent octahedra $V1O_6$, $V2O_6$, and V_3O_6 sharing the edges of their equatorial planes O1–O3 and O2–O4. This block is repeated at the same level by a symmetry center in $\frac{1}{2}, \frac{1}{2}, 0$ located in the middle of the equatorial edge O4–O4*a* of the $V2O_6$ octahedron. These six octahedra (around V1, V2, V3, V1*a*, V2*a*, V3*a*) form an S shaped unit (yellow shaded area), connected via octahedra apices along [0 1 0] forming an infinite ribbon. These ribbons repeated by the twofold helicoidal axis leads to a layer $[V_3O_7]_n$ parallel to the $(\bar{1}\,0\,1)$ plane which repeats with a translation $\vec{t} = -\vec{a}/2 + \vec{c}/2$. The interlayer space is occupied by NH_4^+ cations which ensure the network linkage.

$V1O_6$, $V2O_6$, and $V3O_6$ are rather distorted and vanadium atoms are better depicted as having a CN = 5 + 1. All of them are clearly displaced towards an oxygen apex forming a short bond opposite long bond. In both $V2O_6$ and $V3O_6$ octahedra are observed, vanadyl bonds with V2−O6 = 1.632(4) Å and V3−O7 = 1.612(3) Å while in $V1O_6$ the shortest bond shows a higher value V1−O1 = 1.740(3) Å. All of these bonds point directly towards the layer filled up by NH_4^+ cations, a common feature in vanadium oxide networks containing V^{5+} and V^{4+}. The long V1–O1 bond can be accounted for by the fact that O1 is also bonded to V3, V3−O1 = 2.007(3) Å. These apical oxygen atoms, O1, O6, and O7 are repeated along [0 1 0] forming a triangular prism around the NH_4^+ cations, whose base O6*a*O1O7*d* is shaded in green in Fig. 1. Opposite these short bonds, there are long ones, V1−O2 = 2.207(3) Å, V3−O3 = 2.295(3) Å and the longest and the weakest bonds, V2−O4 = 2.524(4) Å (indicated by dotted lines in Fig. 1). Bonds within the equatorial planes of the VO_6 octahedra evolve normally for V^{5+} and V^{4+} cations, from 1.808 to 2.067 Å. It is to be noted that maximum distortion occurs around the V2 site. The $V2O_6$ and $V2aO_6$ octahedra share the edge O4–O4*a* that is, the hinge of the association of the triple strings of octahedra in order to form the S-shaped ribbon. Potential weakness of this part, associated with V–V repulsions (largest V–V distances, V2−V2*a* = 3.461(2) Å and V1−V2 = V1*a*−V2*a* = 3.363(1) Å) through the large inter-atomic distance of O4−O4*a* = 2.703(9) Å and O4−O2 = O4*a*−O2*a* = 2.712(5) Å compared to O1−O3 = 2.607(5) Å and O2−O5*b* = O2*b*−O5 = 2.504(3) Å and O3−O3*b* = 2.546(3) Å, account for the strong

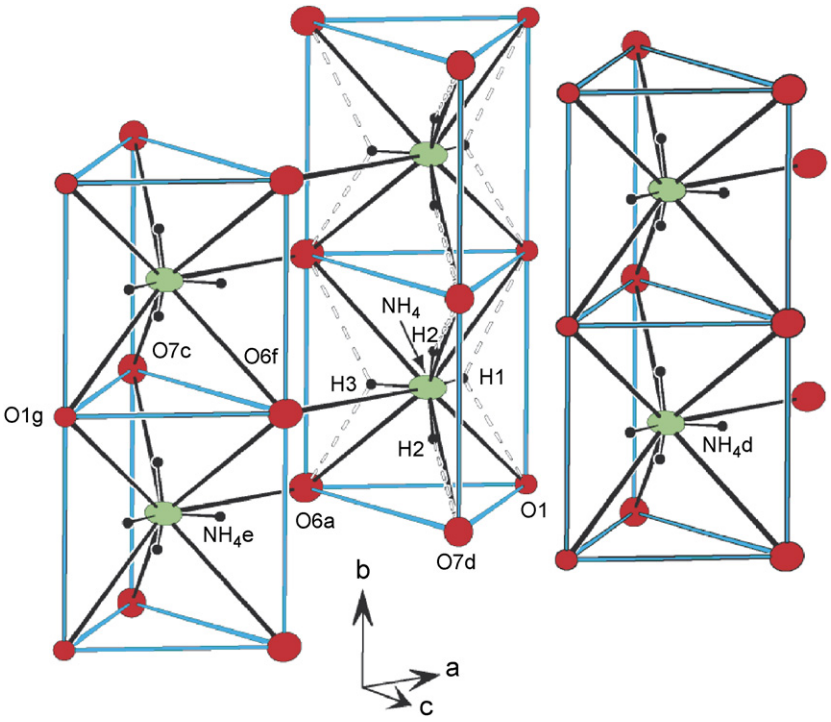

Fig. 2. Environment of ammonium cation in $NH_4V_3O_7$. Symmetry codes are given in Fig. 1.

displacement of V2 inside its octahedron. V2 is pushed towards the fivefold coordination in the form of a square pyramid (SP) $V2O_5$ with the oxygen atoms O2, O6, O4*a*, O5*b*–O5*b*. Similarly deleting the longest bonds V1−O2 = 2.207(3) Å and V3−O3 = 2.295(3) Å, SPs around V1 and V3 are formed. The repulsion between V3 and V1 is the weakest one, V3–V1 inter-atomic distance being only 3.060(1) Å. Along [0 1 0] the V–O bonds are regular with an average $\langle V-O\rangle = 1.942 \pm 0.013$ Å and the V–V distances lie from 2.980(1) to 3.064(1) Å. As previously mentioned, the ammonium ions link the $[V_3O_7]_n$ layers and the environment around NH_4^+ has been defined as a trigonal prism by taking into account the distance lower than 3 Å (N−O1, −O6*a* and −O7*d*, Table 3). However in this environment one distance N−O6*f* = 3.031(7) Å has been neglected. If this distance is included (average distance = 2.922 Å, the ammonium polyhedron may be represented as a monocapped trigonal prism. As depicted in Figs. 1 and 2, two monocapped trigonal prisms related by symmetry with respect to the helicoidal axes (e.g. NH_4 and NH_4e) share a common edge O6*a*−O6*f*. One nitrogen atom is connected to the six oxygen atoms of the previous trigonal prism by hydrogen bonding. The H1 as well as H3 atoms are distant from acceptor atoms O1 and O6*a* by 2.29 and 2.37 Å, respectively, and the angles N−H1…O1 and N−H3…O7*d* are equal to 124.0° and 129.5°. However these data are quite normal since H1 and H3 atoms are bidentate and consequently the four hydrogen bonds are weak. On the other hand H2 is connected only to one oxygen atom O7*d* and the distance H2…O7*d* is 1.96 Å and N−H2…O7*d* being equal to 166.4°, making these two hydrogen linkages relatively strong.

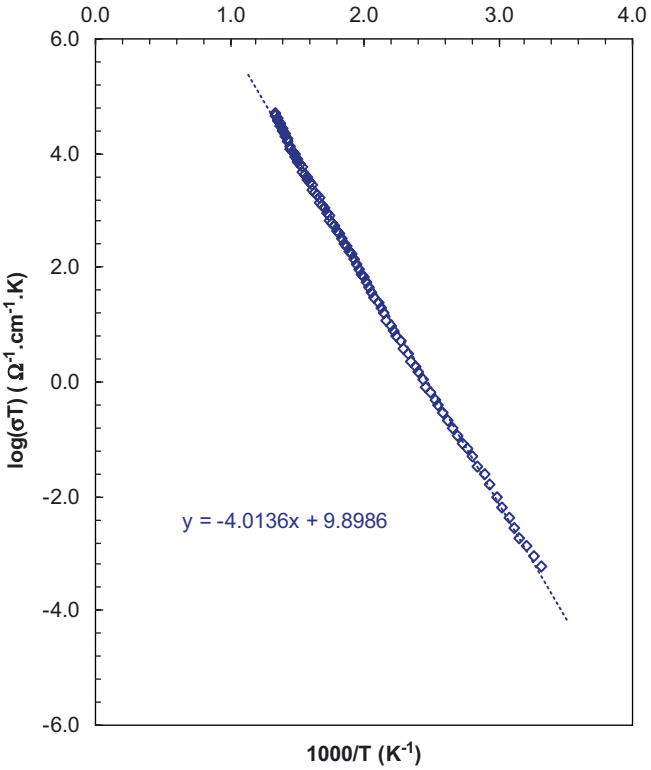

Fig. 3. Arrhenius plot of electrical resistivity of KV_3O_7.

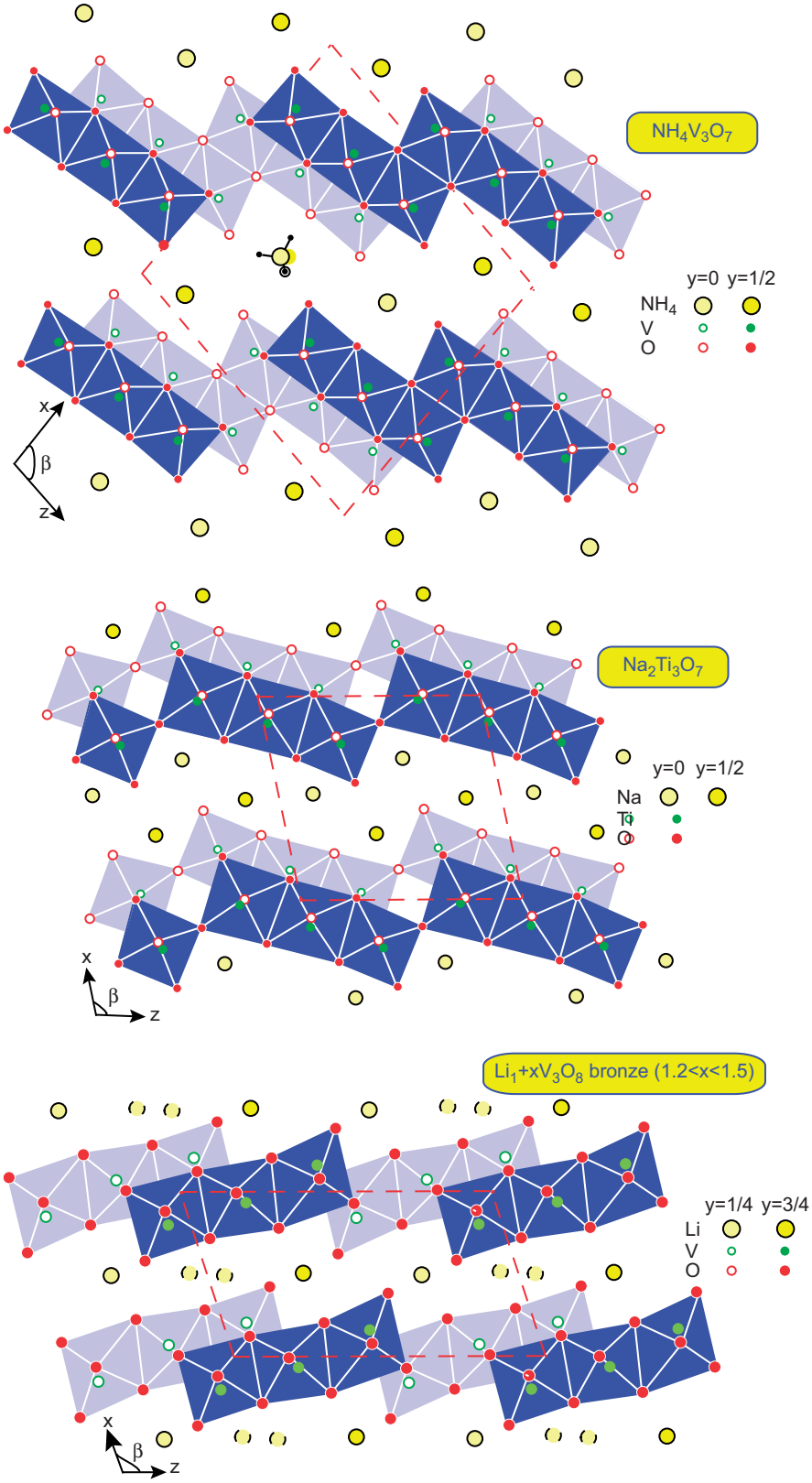

Fig. 4. $NH_4V_3O_7$ compared with phases $Na_2Ti_3O_7$ and $Li_{1+x}V_3O_8$ exhibiting layers built up with the same three octahedra sharing edges on line.

These distances are not uncommon for an ammonium ion: in $(NH_4)_2V_3O_8$ it can be represented as a deformed octahedron with N−O ranging from 2.837 to 2.995 Å (average distance 2.946 Å) [17] while in $(NH_4)V_3O_8$ it is a distorted bicapped trigonal prism with N−O distances ranging from 2.823 to 3.155 Å (average distance 3.018 Å) [24].

3.2. Electrical resistivity

The electrical resistivity ρ of KV_3O_7 between 300 and 750 K indicates that the compound exhibits a semiconductor-like behavior. The temperature dependence of the conductivity σ in a non-metallic state can be modeled by the expression, $\sigma = A\exp(-Ea/RT)$, where Ea is the activation energy. The Arrhenius plot, $\ln\sigma$ vs. $1/T$, is shown in Fig. 3. The activation energy, $Ea = 0.35$ eV falls down in the classical range of the vanadium bronzes 0.3 to 0.5 eV. Typically this value of Ea is expected for the electron hopping process associated with V^{4+} and V^{5+} sites [25].

4. Discussion

As usually occurs with vanadium bronzes, the iono-covalent network is based on the remarkable versatility and flexibility of the V^{5+} and V^{4+} polyhedra coordination which can vary from CN5 to CN6 in the shape of trigonal bipyramids (TBP), square pyramids (SP) and octahedral; V^{5+} also adopts CN4 as tetrahedron VO_4. These CN5 or CN6 coordination schemes are always distorted particularly the CN5 which can evolve from TBP to SP. In $NH_4V_3O_7$ the CN5 + 1 of the vanadium atoms shows an important distortion, the metal atoms being displaced from the equatorial planes respectively by 0.246(2) Å for V1, 0.407(2) Å for V2 and 0.415(2) Å for V3. If the long bond V2–O4 is omitted the triple strings of octahedra via O4–O4*a* edge allows a structure description in terms of double strings of octahedra $V1O_6$ and $V3O_6$ connected via chains of $V2O_6$ SP. It allows the sextuple ribbon to breathe up to a value of the V1O4V2*a* angle equal to 180°. This possibility, even more restricted, could be similar to the bronze $Li_{1+x}V_3O_8$ in which the longest distance around 2.86 Å allows to describe it as double ribbons linked by SP (a projection of this structure with its three VO_6 octahedra edge shared is given in Fig. 4). Such a capacity does not exist in the structure of $Na_2Ti_3O_7$ [26] where the TiO_6 octahedra are more regular and the triple ribbons firmly connected at the same level by corner sharing, creating a continuous wavy line, while the two other phases show a continuity after repeating by a shift of $b/2$.

There is a question concerning the charge distribution in the $(V_3O_7)_n$ layer which contains one V^{5+} for two V^{4+}, $NH_4V^{5+}V_2^{4+}O_7$. Are formal charges localized? This problem was easily resolved in the $(NH_4)_2VO(V_2O_7)$ phase where a clear distribution with one V^{4+} in a square pyramid VO_5 (the group VO^{2+}) and two V^{5+} in pyrovanadate group V_2O_7. Here such clear distribution was not expected. To assess the possible distribution of charges in VO_6 octahedra we performed a bond–valence sum analysis according Brown and Altermatt [27]. To make such calculations an r_0 value for V^{n+} was extrapolated taking into account the ratio $V^{5+}/V^{4+} = \frac{1}{2}$; it yields $r_0 = 1.7925$ ($\langle n = 4.333\rangle$). The calculated valence in the two types of polyhedra, i.e. square pyramid and octahedron, are summarized in Table 4. According to this calculation, there is an indication that V^{4+} should normally occupy, in majority, the V1 and V3 sites, V1 being the most favorable. This suggestion seems to be supported by the distribution of V–O bond distances which do not exhibit the presence of a V=O vanadyl group and the smallest gap between the longer and shorter V–O bond, 0.467 Å. The V3 site is adapted to a mixed vanadium valence. The V2 site with its large gap between the bonds, 0.892 Å, and the large V2–V2*a* = 3.461 Å distance, indicating a noticeable charge repulsion together with the highest bond valence calculation, seems to be more favorable to V^{5+}.

Table 4
Average ⟨V–O⟩ bond lengths (Å), bond valence (with its formal charge) and $d_\perp$ (Å) distance of *V* to the basal plane in VO_5 SP in various vanadium oxide compounds

Phases	⟨V–O⟩ Å	Bond valence	$d\perp$ (Å) in SP	References
V_2O_5	1.823	$V^{5.1+}$	0.470	[6]
$\gamma LiV_2O_5-V_1$	1.876	$V^{4.4+}$	0.539	[28]
$\gamma LiV_2O_5-V_2$	1.826	$V^{4.9+}$	0.636	
α' NaV_2O_5	1.852	$V^{4.6+}$	0.562	[29]
MgV_2O_5	1.894	$V^{4.0+}$	0.666	[30]
	1.895–CN5	$V^{3.9+}$–CN5		
$NH_4V_3O_7-V_1$	1.947–CN6	$V^{4.4+}$–CN6 ⟨4.15⟩	0.246	This work
	1.873–CN5	$V^{4.3+}$–CN5		
$NH_4V_3O_7-V_2$	1.981–CN6	$V^{4.8+}$–CN6 ⟨4.55⟩	0.407	This work
	1.897–CN6	$V^{4.1+}$–CN5		
$NH_4V_3O_7-V_3$	1.963–CN6	$V^{4.6+}$–CN6 ⟨4.35⟩	0.415	This work

However, there is no evidence, as in the case of double strings of VO_5 square pyramids of the mixed vanadium–molybdenum bronze $K_{2-x}Mo^{6+}_{x+y}V^{5+}_{8-x-2y}V^{4+}_yO_{21}$ [2] where the calculated valence was 4.97, clearly indicating the presence of V^{5+}. This phase $NH_4V^{5+}V_2^{4+}O_7$ must be considered as a mixed valence compound, while $Li_{1+x}V^{5+}_{3-x}V^{4+}_xO_8$ is a bronze phase (non-stoichiometry in lithium).

Appendix A. Supplementary data

Further details of the crystal structure can be obtained from the Fachinformationszentrum Karlsruhe, 763344 Eggenstein-Leopoldshafen, Germany (fax: +49 7247 808 666; E-mail: crysdata@fiz-karlsruhe.de) on quoting the CSD-number 417589.

References

[1] A.D. Wadsley, Acta Cryst. 8 (1955) 695–701.
[2] P. Millet, C. Gasquères, J. Galy, J. Solid State Chem. 163 (1998) 210–217.
[3] A.D. Wadsley, Acta Cryst. 10 (1957) 261–267.

[4] M. Morcrette, P. Rozier, L. Dupont, E. Mugnier, L. Sannier, J. Galy, J.M. Tarascon, Nat. Mater. 2 (2003) 755–761.
[5] P. Rozier, S. Lidin, J. Solid State Chem. 172 (2003) 319–326.
[6] R. Enjalbert, J. Galy, Acta Cryst. C42 (1986) 1467–1469.
[7] S.R. Batten, R. Robson, Angew. Chem. Int. Ed. 37 (1998) 1460–1494.
[8] T. Chirayil, P.Y. Zavalij, S. Whittingham, Chem. Mater. 10 (1998) 2629–2640.
[9] H. Li, M. Eddaoudi, M. O'Keeffe, O.M. Yaghi, Nature 402 (1999) 276–279.
[10] A.K. Cheetham, G. Férey, T. Loiseau, Angew. Chem. Int. Ed. 38 (1999) 3268–3292.
[11] T.M. Reineke, M. Eddaoudi, M. O'Keeffe, O.M. Yaghi, Angew. Chem. Int. Ed. 38 (1999) 2549–2593.
[12] P.J. Hagrman, D. Hagrman, J. Zubieta, Angew. Chem. Int. Ed. 38 (1999) 2638–2684.
[13] J.L.C. Rowsell, O.M. Yaghi, Micropor. Mesopor. Mater. 73 (2004) 3–14.
[14] C. Brouca-Cabarrecq, A. Mohanu, P. Millet, J.C. Trombe, J. Solid State Chem. 177 (2004) 2574–2582.
[15] J.C. Trombe, J. Jaud, J. Galy, J. Solid State Chem. 178 (2005) 1094–1103.
[16] F. Duc, S. Gonthier, M. Brunelli, J.C. Trombe, J. Solid State Chem. 179 (2006) 3591–3598.
[17] K.-J. Range, R. Zintl, Z. Naturforsch. Teil B Anorg.: Chem. Org. Chem. 43 (1988) 309–317.
[18] F.R. Theobald, J.G. Theobald, J.C. Vedrine, R. Clad, J. Renard, J. Phys. Chem. Solids 45 (1984) 581–587.
[19] J. Galy, A. Carpy, Acta Cryst. B31 (1975) 1794–1795.
[20] F. Belaj, A. Basch, U. Muster, Acta Cryst. C56 (2000) 921–922.
[21] P. Coppens, in: F.R. Ahmed, S.R. Hall, C.P. Huber (Eds.), Crystallographic Computing, Copenhagen, Munksgaard, 1970, pp. 255–270.
[22] A. Altomare, G. Cascarano, C. Giacovazzo, A. Guagliardi, M.C. Burla, G. Polidori, M. Camalli, J. Appl. Cryst. 27 (1994) 1045–1050.
[23] G.M. Sheldrick, SHELXL-97, Program for the Refinement of Crystal Structures, University of Göttingen, Germany, 1997.
[24] B.Z. Lin, S.X. Liu, Acta Cryst. C55 (1999) 1961–1963.
[25] A. Casalot, D. Lavaud, J. Galy, P. Hagenmuller, J. Solid State Chem. 2 (1970) 544–548.
[26] S. Andersson, A.D. Wadsley, Acta Cryst. 14 (1961) 1245–1249.
[27] I.D. Brown, D. Altermatt, Acta Cryst. B41 (1985) 244–247.
[28] J. Galy, J. Darriet, P. Hagenmuller, Rev. Chim. Miner. 8 (1971) 509–522.
[29] M. Isobe, Y. Ueda, J. Phys. Soc Jpn. 65 (1999) 276–279.
[30] P. Millet, C. Satto, P. Sciau, J. Galy, J. Solid State Chem. 136 (1998) 56–62.